Atmospheric Environment Vol. 15, No. 10/11, pp. 2079–2090, 1981
Printed in Great Britain.

0004-6981/81/102079-12 $02.00/0

LARGE FIRE WINDS, GASES AND SMOKE*

THOMAS Y. PALMER†
SWETL, Inc., PO 278 Fallbrook, CA 92028, U.S.A.

(*First received* 19 *September* 1980)

Abstract—Experimental, free-burning wood fires larger than 5 ha were similar in convection column volume after the initial buoyant, ring-vortex rose from the ground. The fire generated strong vorticity patterns which propagated upward into the convection column. The rotation suppressed lateral entrainment and mixing after the buoyant vortex ring had passed. The maximum height of the convection column was determined by vertical wind shear. Maximum smoke, complex hydrocarbon concentrations, combustion gas concentrations, oxygen depletion and visibility reduction and radiation extinction occurred during the first 210 s of the fires.

1. INTRODUCTION

The multi-national large fire program, Project Flambeau, studied the effects and behavior of large fires from 2 to 20 ha in size. Approximately 25 experiments were burned between 1964 and 1975. The experimental fuels consisted of piles of pinyon pine and juniper, winrows of heavy, large sized pieces of brigalow with little fine fuel and areas of southern California chaparral which were mostly fine fuel. These fires were ignited simultaneously over the whole area in light wind conditions. This ignition pattern produced vertical convection columns which converged to a small cross-section in the lower 100 to 200 m, then diverged and rose at a fairly uniform rate to a height usually in excess of 1000 m. This smoke column behavior was different from either low or moderate intensity fire smoke columns burning under strong wind conditions. The smoke plume from these latter type fires remains more attached to the terrain and the physical mechanisms governing smoke dispersion is apparently quite different from the large fire convection column. The experiments and some of the results are described in what follows.

2. INSTRUMENTATION

Although there was speculation about the behavior of large fires for many years following the 1924 Tokyo fire and the World War II city conflagrations, quantitative measurements of large, free-burning fires had not been made prior to the 1964 Project Flambeau experimental fires. New instrument systems were developed for use inside these fires. These included fixed-axis, fire-resistant, water cooled anemometers similar to those shown in Fig. 1 (Palmer and Northcutt, 1972), aspirated and radiation-compensating thermocouples (Palmer, 1971), continuous flow calorimeters, fuel weight platforms (Murray *et al.*, 1971), and life support and escape studies. These instruments were installed inside large, square fuel arrays such as the one shown in Fig. 2. These arrays ranged from 2.5 to 25 ha. The temperature and wind instrumentation were mounted on towers up to 30 m high, in a number of configurations, while the other instruments were placed in various locations inside the fire perimeter. The electrical signals were brought out of the fire area by an extensive net of underground wiring to a recording center where data was recorded every 10 s.

Outside the fire perimeter, instrumentation included vertically mounted flat-plate, total radiometers, pulsed-Doppler radars (Lhermitte, 1969), smoke visibility measurements, gas sampling and analysis apparatus, infra-red spectral scanners and imagers and other equipments. Still and cine photographic coverage was extensive and carefully timed. Most camera sites were located by a first order survey. Each fire was started with uniformly distributed napalm blivets and grenades, usually ignited simultaneously by electrical means.

3. COMBUSTION PRODUCTS

Fuel consumption

Burning of the wood fuels was measured by their weight loss, and was converted to energy release rates on the basis of calorimetric measurements of fuel from the individual plots. Figure 3 shows the energy release rates for the Operation Euroka fire (Williams *et al.*, 1970) and the Project Flambeau fires in the U.S.A. For comparative purposes, the energy output of the Meteotron Facility (Benech, 1976; Church *et al.*, 1980) are included.

Fuel consumption measurements in the fire were made by: (1) placing several piles of the pinyon-juniper fuel on the 15 m × 15 m weighing platforms and (2) constructing carefully assembled fuel arrays of seized wood pieces designed to have a uniformly reproducible fuel size distribution, fuel bed porosity

* Paper presented at the Symposium on Plumes and Visibility: Measurements and Model Components. Grand Canyon, Arizona, U.S.A. 10–14 November 1980.

† Some the experimental work was performed at the U.S.D.A. Forest Service Riverside Forest Fire Laboratory.

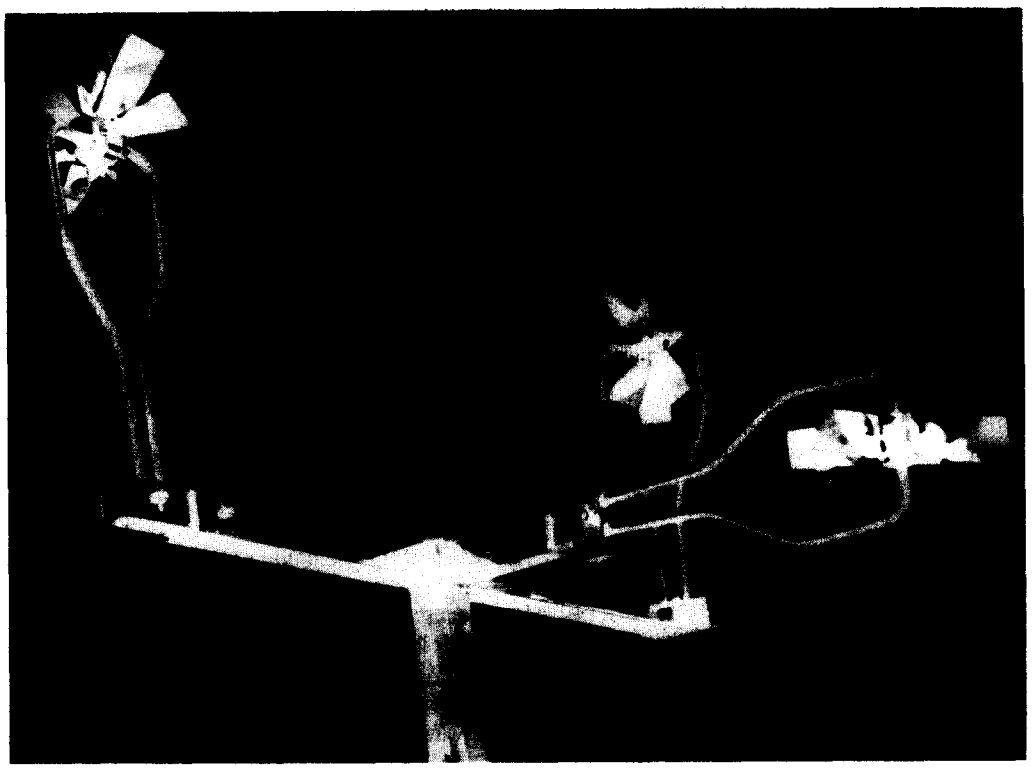

Fig. 1. Water cooled anemometers such as used in the Project Flambeau fires had a starting speed of 0.25 $m\,s^{-1}$ and a response length of 1 m.

and total mass similar to that of the basic piles on the weighing platforms. The fabricated piles were designed to correlate burning rates in these fires with small scale laboratory fires.

Analysis of the 12 Project Flambeau weight loss experiments in the U.S.A. showed that most of the fine materials were burned in the first 2–5 min. This time interval was the period of maximum production of volatile complex organic compounds. Larger sized wood (2 cm and larger), was the principal fuel burned after the peak energy release rates in these experiments. The Project Euroka fire in Australia fuel was principally brigelow, a heavy dense hardwood with a high mineral content. In addition the Euroka fuel beds were rearranged so that there was little fine material. For these two reasons, the peak combustion rates of Project Euroka were considerably later than those of the U.S.A. fires.

Combustion gases

Combustion gases were sampled through intake tubes at the 1 and 2 m levels located between piles of burning fuel. The combustion gases were drawn through pipes to a gas analysis trailer near the edge of the fire. Grab samples were also obtained by use of remotely actuated evacuated cylinders. Typical combustion gas concentrations are shown in Figs 4 and 5. Typically, during the first 3 min, oxygen concentrations decreased sharply—in extreme cases as low as 4% with a concomittant increase in combustion gas concentrations. Carbon dioxide concentrations as great as 4% occurred, while water vapor reached levels as great as 8% (not relative humidity). Concentrations of the complex hydrocarbons were apparently produced and dispersed in the same way as carbon dioxide, but their correlation to oxygen concentrations was poor. Gas chromatographic analysis of smoke identified hundreds of complex hydrocarbons (some of them photochemically active) in concentrations ranging from 5000 to 20 000 ppm.

The Operation Euroka fire developed a charcoal combustion phase after sunset and continued smouldering for over 18 h. High carbon monoxide levels developed inside the fire perimeter during the night under a shallow temperature inversion.

Combustion particulates

Solid particulates in these fires were sampled by a thermal precipitator. They ranged from 2 to 10 μm in over-size and consisted mainly of mineral soil and carbon particles. In some cases remanents of the physiological structure of the wood could be identified. Typical observed concentrations were 1 $mg\,m^{-3}$, but these were obviously not characteristic of the convection column because of the location of the samplers between the aisles.

Liquid particle sampling was not completely successful. Samples on millipore filter paper showed them to be light to dark brown material, tarry in consistency, which were soluable in acetone. Apparently, they were

Fig. 2. The large fuel arrays of Project Flambeau contained 18 tons of mixed Pinyon–Juniper trees in 15 m × 15 m piles separated by 7.5 m aisles.

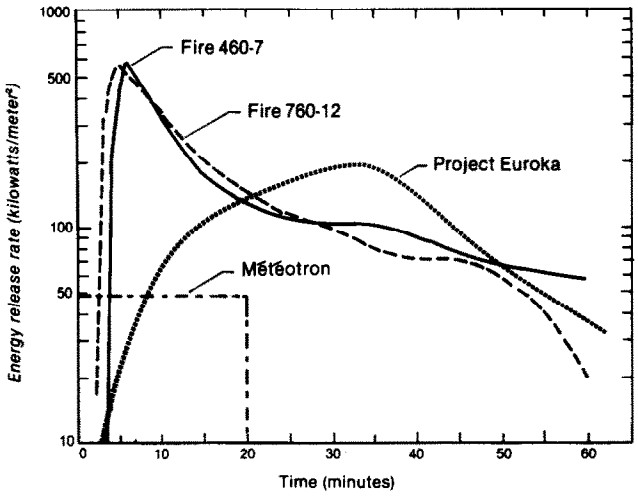

Fig. 3. Energy release rates per unit area for various fire experiments. Fire 7 was 12 ha, Fire 12 and Operation Euroka were 20 ha. The Meteotron is 2 ha.

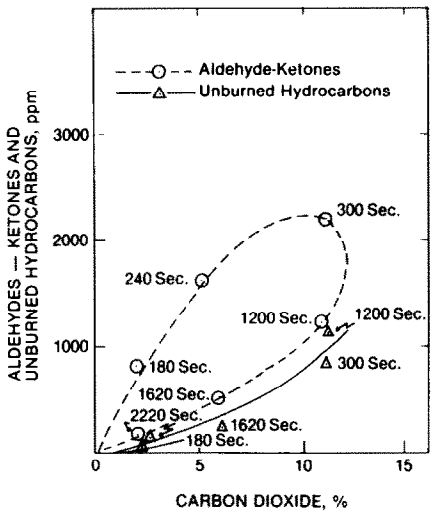

Fig. 4. Most of the complex pyrolytic hydrocarbons were produced in the first few minutes of the Project Flambeau fires.

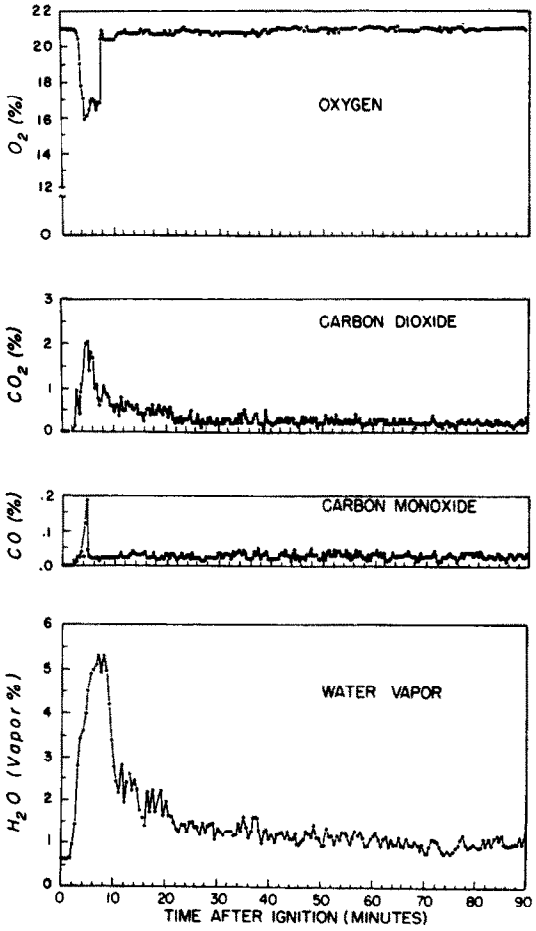

Fig. 5. Typical gas concentrations at the 1 m level during Project Flambeau Fire 12.

complex tars and sugars produced by the pyrolysis of the wood, which combined with the water of combustion to produce matrix particles and solution drops. The thermal precipitators were operated at 100°C which melted the drops and caused them to form a thin film on the slide. Attempts to examine the millipore paper samples under an electron microscope caused the drops to collapse or evaporate under the vacuum.

Burning wood produces about one part water per part of dry wood. Addition of this water of combustion and the absorbed water in the wood to the air of the convection column did not alter the lifting condensation level from that of the ambient atmosphere. This indicates that most of the water from the wood went to form liquid smoke particles which form very near the burning fuel. Tracer elements suitable for neutron activation analysis were placed in some of the fires. They were not detected at ground level within 8 km of the fires.

Although the centrifugal forces of firewhirls are

Fig. 6. Observations of street signs in Project Flambeau Fire 12 by observers at the edge of the fire. Note the effects of the strong downdraft on the fire.

strong enough to eject pieces of wood 5 cm dia. and 1 m long, the updrafts were strong enough to carry most of the smoke and particulates into the convection column.

4. VISIBILITY, RADIATION AND EXTINCTION

As illustrated in Fig. 6, visibility measurements in the Project Flambeau fires were made by observing typical San Francisco street signs mounted above 102 cm × 46 cm white panels 2 m above the ground. The measurement results are shown in Fig. 7. The dashed lines enclose periods when the visibility was less than the distance to the nearest sign. It is apparent that changing wind patterns within the fire greatly influenced the visibility.

A typical infra-red spectral scan of the flame and gas emission radiant intensity is illustrated in Fig. 8. This data shows that the radiation from the flames is that of a 1500 K (2200° F) blackbody, with strong absorption by the combustion gases. This temperature is within the range of measured temperatures of free burning wood fires (Palmer, 1971).

Total radiative output from the fires was measured by vertical, flat-plate radiometers mounted 30 m from the fire edge and 3 and 15 m above the ground. The curve of radiative output as a function of time closely resembles the form of the energy release curves of Fig. 3. Peak radiant flux on the instruments ranged from 16 to 66 $W m^{-2}$, with the variability depending upon wind direction and flame heights.

Palmer (1976) performed a parametric integration of the transmission of solar radiation and radiation from Fire 10 through the convection column to the flat-plate radiometers over similar paths. As illustrated in Fig. 9, maximum extinction of the total radiation occurred about $2\frac{1}{2}$ min after ignition and decreased rapidly after that time. Values of the average extinction coefficient ranged from 1 to 10^{-2} km^{-1}, as compared to visibilities on the order of 100 m.

5. FIRE WINDS, TEMPERATURES AND CONVECTION COLUMNS

Winds inside the combustion zone of a large fire are important to air quality and visibility because they

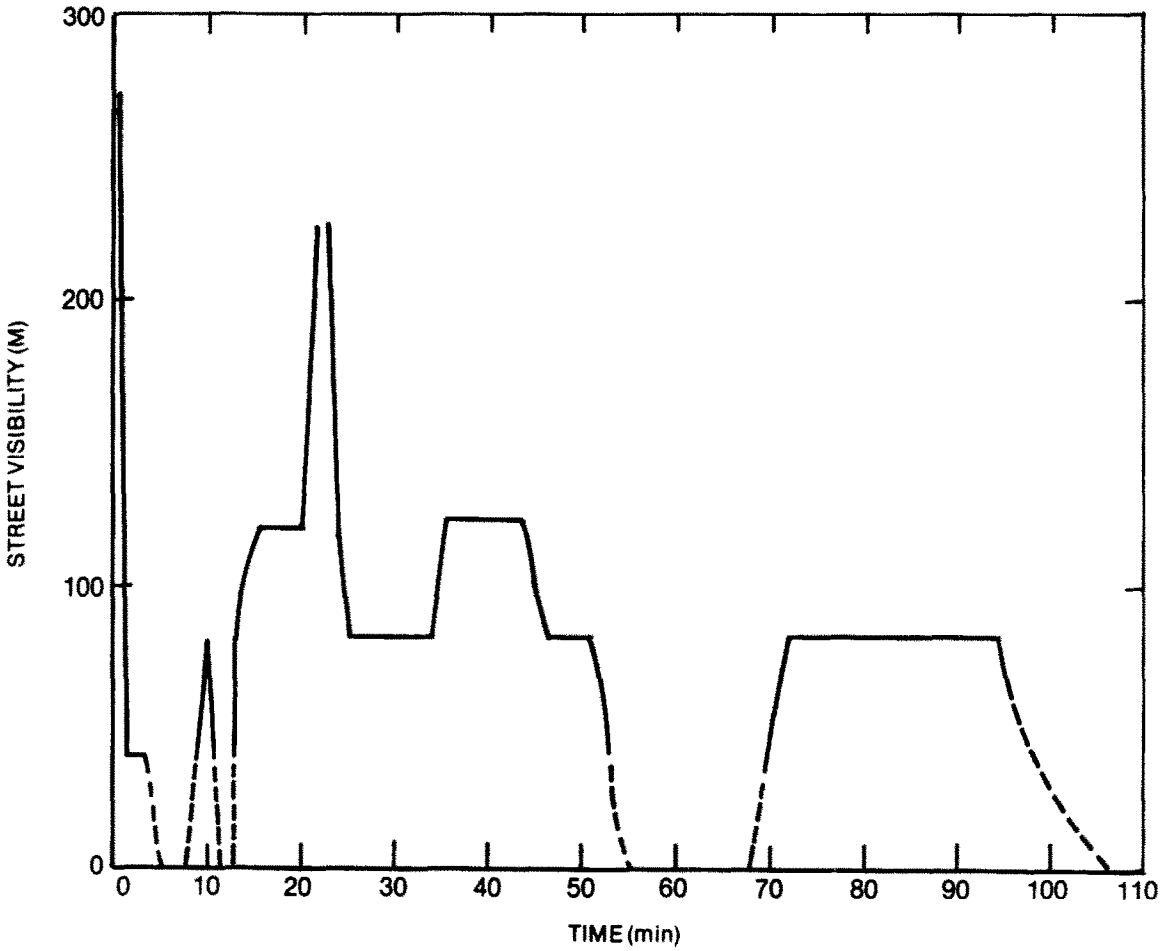

Fig. 7. Visibility measurements in Fire 12 were made both visually and photographically of street signs with identical results. The Sun was behind the observers.

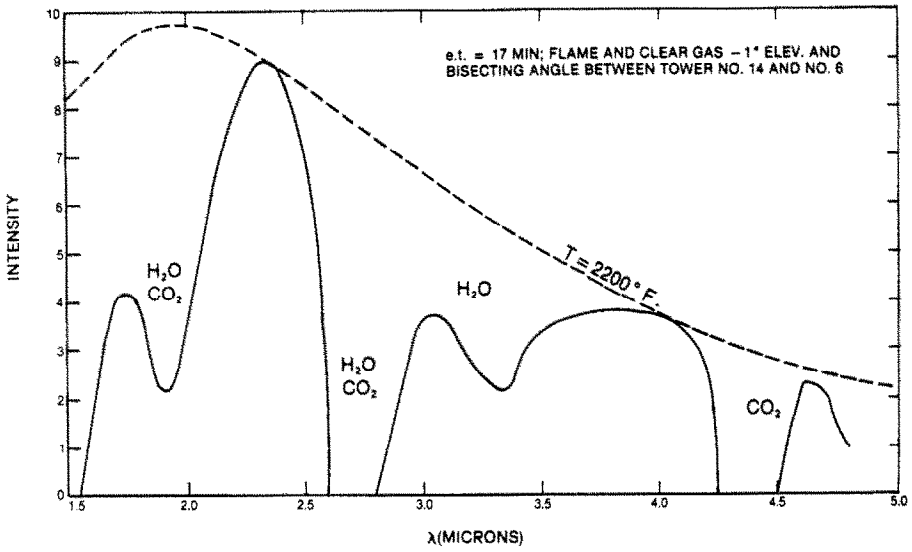

Fig. 8. A typical scan of the radiant intensity as a function of wave length of Project Flambeau Fire 12, shows strong absorption by water vapor and carbon dioxide.

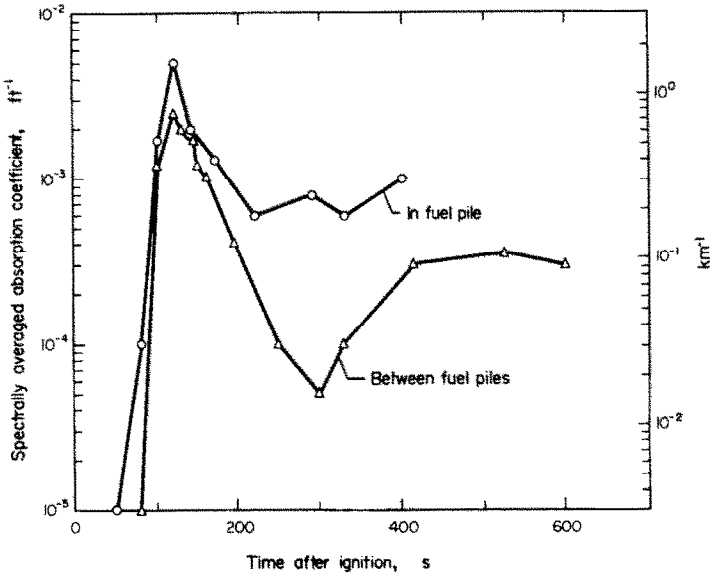

Fig. 9. Range of possible values of the spectrally averaged absorption coefficient as a function of temperature inside the fire area.

raise mineral soil as dust, loft pieces of solid fuel, and influence the rates of burning and the kinds of pyrolytic combustion products produced.

Fires are different from ordinary atmospheric thermals because the combustion of the fuel acts as a continuous sink of air, and at the same time, the fire acts as a continuing, intensive source of heated air at the base of the convection column. This should be compared to the transitory pulse of warm air at the base of an atmospheric thermal and the extensive energy source due to condensation in a natural water cloud.

The lower 100 to 200 m of the Project Flambeau convection columns contracted because of the inflow of the air to the fire. This inflow was horizontal at ground level, but contained a considerable downward component aloft. For instance, attempts to raise a 500 g helium filled balloon at the left hand corner of Fire 6 (shown in Fig. 13) were unsuccessful because the balloons were carried downward into the flames. Yet, the fire's hot gases moved upward into the rising convection column. This complex flow formed a zone of intense turbulence and mixing. In addition the fire winds usually had rotational circulation which propa-

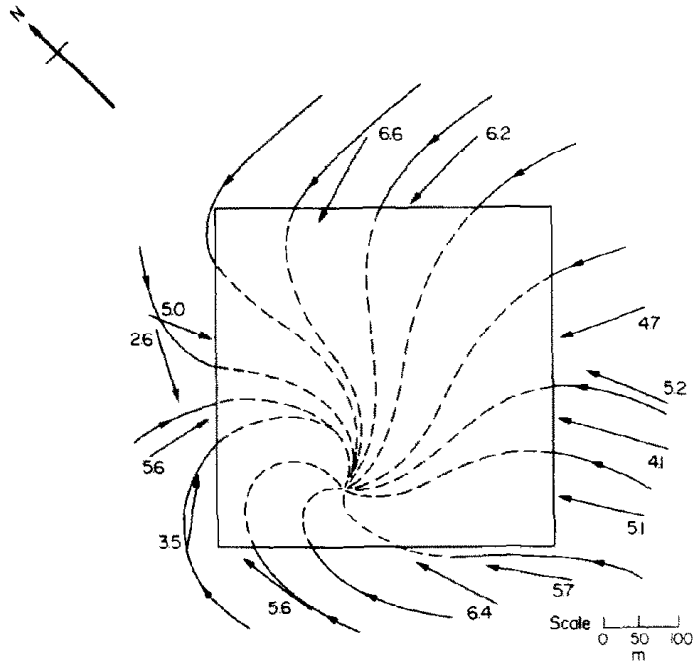

Fig. 10. Vector winds at two meters in the Operation Euroka fire, 40 min after ignition, together with inferred streamlines.

gated into the convection column. This vorticity later influenced the rates of smoke and combustion gas dilution because of decreased entrainment.

Fire winds

Winds in these large fires circulated in two principle patterns. They were: (1) the isolated single line vortex shown in Fig. 10 of the Operation Euroka experimental fire and Project Flambeau Fire 10 and (2) the more common dual vertical line vortex pattern illustrated in Figs 11 and 12.

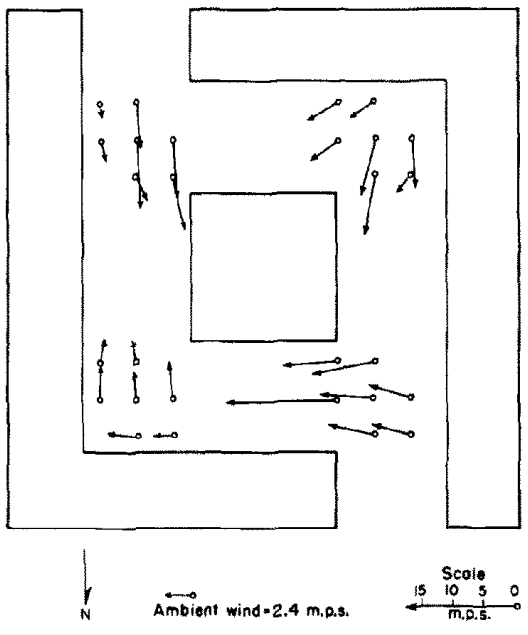

Fig. 11. Interior wind vectors of Project Flambeau Fire 6 showing double vortex pattern.

The internal circulation pattern of these fires depended upon the time between ignition and peak burning rate, the burning pattern and local terrain. A slow buildup of fire intensity favors the formation of the single line vortex as shown in Fig. 13, as does a fire ignited with wings to guide the inflow into a central burning area in a spiraling manner. Fire 10 was ignited in this pattern as an extension of laboratory experiments which showed that such wings could cause a large firewhirl. It required 2 h of burning for this pattern to generate a 12 ha firewhirl, which scoured the ground clean, removing all material smaller than about 1 cm dia. Maximum measured winds were 56 m s^{-1}. The experimental area is still bare of significant vegetation 12 years later.

The Operation Euroka firewhirl required about 30 min to develop. Its maximum winds were 20 m s^{-1}, with a central pressure depression of 1.8 millibars. My measurements of winds in other relatively weak firewhirls have observed vertical winds of 70 m s^{-1} and downdrafts of 50 m s^{-1} across the flame front—a distance of about 2 m.

It seems assured that the firestorm phenomena is associated with the isolated single line vortex. Lofting of significant amounts of large material requires the stronger winds associated with this circulation rather than the more common indraft winds and line vortex pair.

Fire temperatures

Temperatures in the flames of free-burning, wildland fires in which the air has not been preheated were

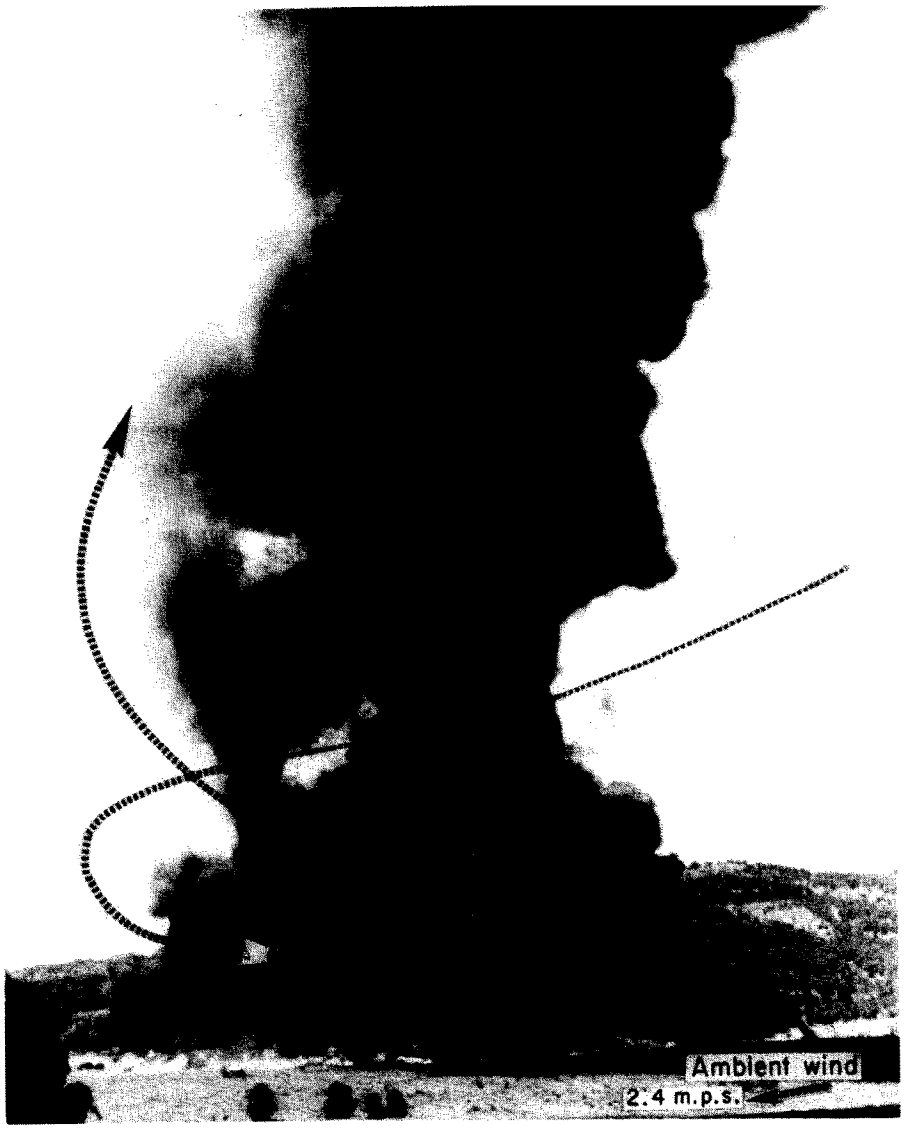

Fig. 12. Exterior of fire 6. Smoke bombs at various altitudes outside the fire followed these trajectories.

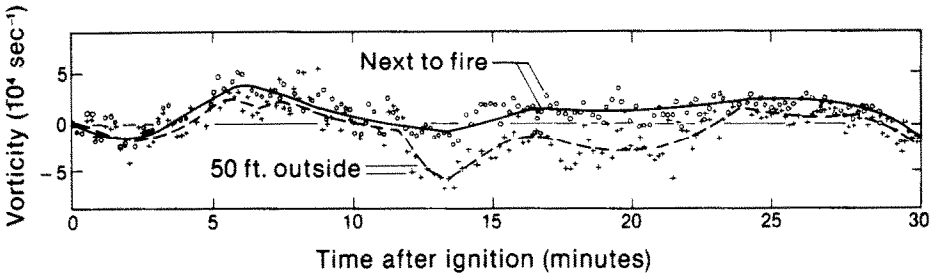

Fig. 13. Vorticity around the perimeter of Fire 10 at the 1.5 m level. Orthogonal anemometers were spaced on a 15 m × 45 m grid.

about 1600 K. Turbulent flame temperature spectra, normalized with the height and ambient wind speed had a $-7/3$ds slope on a logarithmic plot, in agreement with the theory for the spectra of a passive additive in turbulent flow, within the inertial subrange when energy is added to the flow (Tennekes and Lumley, 1972). Intense mixing of the inflowing ambient air with the combustion gases reduced temperatures rapidly

with altitude above the flames (1000° C in 15 m). Excess temperatures inside the convection column, 200 m above the flames were only a few degrees above ambient temperatures.

Convection columns

The atmospheric temperature profiles of Fig. 14, show that these fires were burned under a wide range of atmospheric stability, ranging from extremely stable (with snow on the ground) in Fire 14 through conditionally unstable in Fire 12 and Operation Euroka to absolutely unstable in Fire 7. The rise of the convection columns is shown in Fig. 15. Initially, a bubble of hot combustion gases built up over the fires and expanded out of the fire area as shown in Fig. 16. When this bubble had developed sufficient buoyancy to overcome surface drag, the hot gases broke loose from the ground and rose as a vortex ring. The rate of rise of the initial vortex and half-angle of spread, α of the convection column depended upon the internal circu-

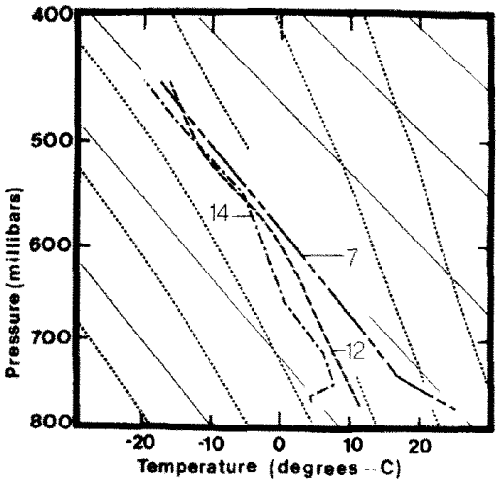

Fig. 14. Pseudo-adiabatic plots of atmospheric temperature and pressure for some Project Flambeau fires, show stability ranges from absolutely stable to absolutely unstable.

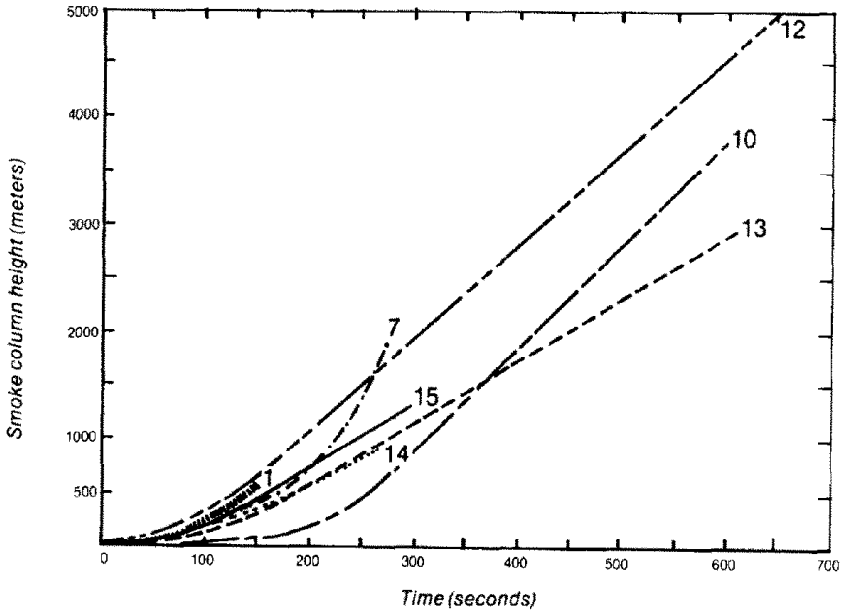

Fig. 15. Most of the Project Flambeau test fire convection columns rose at a constant speed after the initial breakaway from the ground. Fire 7 continued to accelerate because the atmosphere was absolutely unstable. All columns stopped rising when they encountered vertical wind shear.

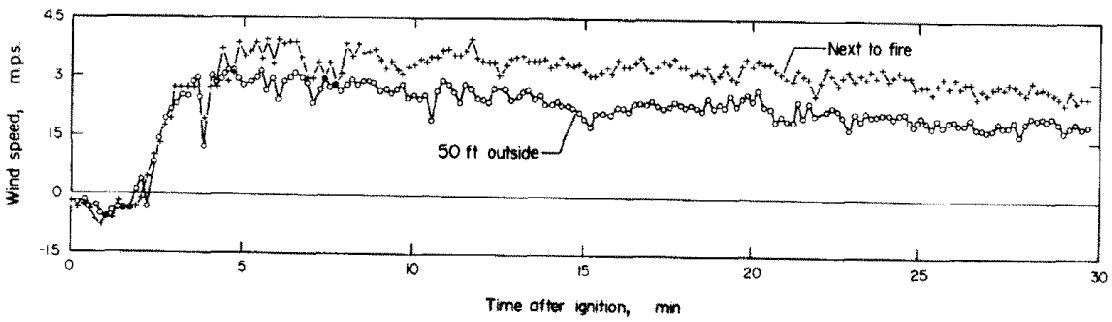

Fig. 16. Net flux into Project Flambeau Fire 10 at the 1.5 m level as measured by orthogonal anemometers spaced around the fire as in Fig. 13.

Table 1. Half angles of spread of convection columns in Project Flambeau and Operation Euroka fires

Fire	Size (ha)	Half-angle (deg)	Atmospheric conditions
12	20	5.2	Conditionally unstable
Operation Euroka	20	14	Conditionally unstable
14	16	2.5	Strongly stable
10	12	3.5	Conditionally unstable
7	12	7.8	Absolutely unstable
13	12	12.7	Stable
6	6	7.6	Neutral
15	2	12.5	Stable
5	2	0	Neutral
2	2	2.7	Conditionally unstable

lation of the vortex K_0 and the buoyancy force, f as (Turner, 1973)

$$\alpha = \text{constant} * \frac{f}{K_0^2}. \quad (1)$$

The rate of rise of the vortex ring, $U_z(\mathrm{m\,s^{-1}})$ apparently depended upon the lapse rate* of ambient temperature, dT/dh ($^\circ\mathrm{C\,m^{-1}}$) in the lower 100 m as (Palmer, 1975)

$$U_z = 1.15 \exp\left(153\frac{dT}{dh}\right). \quad (2)$$

As illustrated in Table 1, the half-angle of spread was quite variable for these experiments even though the energy release rates per unit area were very nearly the same, while the variation in surface roughness was small between the fires because of the similarity of the plots and vegetation. This variability of half-angle may be related to the constraint shown in Fig. 17, that the volume of the convection column for all of the fires in the United States be the same after the initial breakaway of the initial bubble of hot gases.

In every case (even in the absolutely unstable ambient atmosphere of Fire 7) the initial bubble vortex rose until it encountered a region of vertical wind shear. At this level the vorticity couple caused the upwind side of the vortex to weaken and stop rising. The downwind portion of the vortex decelerated and moved horizontally with the upper level winds. During the analysis of the smoke columns, it became clear that the exterior form of the convection column at a particular altitude was determined by the initial vortex bubble as it passed that altitude and that the exterior shape of the vertical portion of the convection column subsequently changed little over periods as long as 30 min. This implies that there is little entrainment into the rising core of the convection column.

Below the initial ring vortex, the convection column consisted of one or two vertical line vortices based in the fire. In the single line vortex fire, the convection column shrank to about two-thirds of the diameter of the fire at the base within about 200 m above the fire.

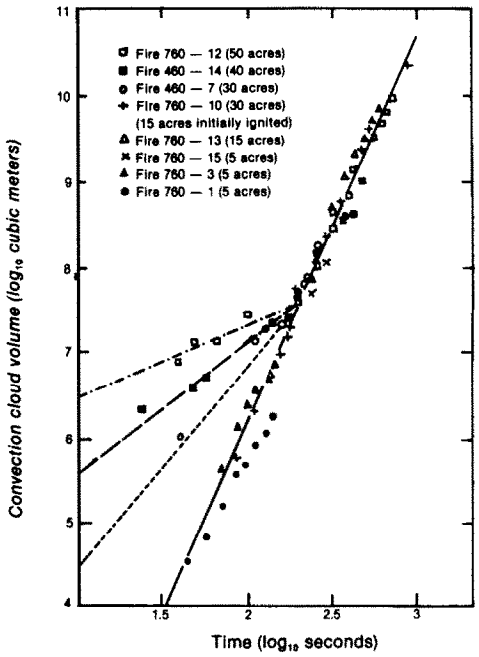

Fig. 17. Photogrammetric analysis of Project Flambeau fire convection columns shows that their volumes were the same after the breakaway of the initial bubble from the ground. Volumes are accurate to about 1%.

For instance pulsed Doppler observations of Fire 10 (Lhermitte, 1969) showed the diameter of the rising column was 200 m at an elevation of 600 m above the fire which was 300 m on a side. The upward velocity inside the core of the convection column was 9 $\mathrm{m\,s^{-1}}$— the same as the rise rate, while the velocity profile across the convection column had a 'top-hat' shape.

The double-vortex fire illustrated in Fig. 18 was more usual. The vortex pair was driven by a downward descending jet which supplied a major part of the air used in combustion. In Fire 12, this downward jet was 15 $\mathrm{m\,s^{-1}}$. Its effect in knocking down the flames is noticeable in Fig. 7. The location of the bases and strength of the line vortex pairs was not consistent in time. Such line vortex pairs are stable and exchange little mass with their environment. This characteristic is apparently preserved even after the convection

* Note added in proof: the normal lapse rate of atmospheric temperature is a decrease with height, thus dT/dh is intrinsicly negative.

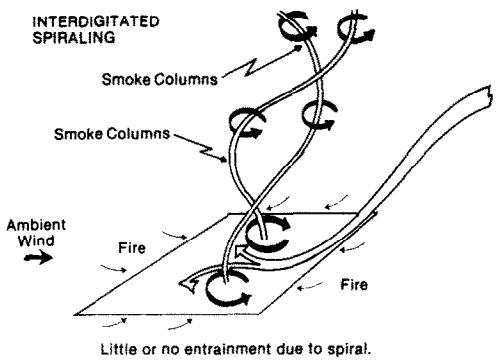

Fig. 18. Model of an interdigitated vortex pair which is driven by a downward jet into the fires center. The jet may come from either upwind or downwind and can spiral about the convection column as in Fig. 12.

column is bent over, since the smoke column of Fire 10 displayed little lateral or vertical dispersion for the 100 km it was tracked by aircraft.

6. MODELS

Extensive studies designed to formulate a fire model based upon the work of Morton *et al.* (1956) and others were unsuccessful in developing a model which was consistent between any two experimental fires. This lack of agreement probably occurs because of the implicit model assumptions of horizontal flow during lateral entrainment, the effects of the vertical line vortices and of wind shear in the atmosphere. These assumptions were not congruent with these experiments.

Computer simulations using two-dimension convective models based upon stream functions and the Boussinesq approximation, using a positive coefficient of eddy transfer for heat, momentum and water vapor were successful in simulating the development of the heat bubble and the vortex ring of the first phases of the fire. The model broke down shortly after the vortex ring left the ground.

7. CONCLUSIONS

Large freely burning fires generate relatively large amounts of complex gaseous hydrocarbons in the first three minutes of burning. These gases are concentrated in a bubble of hot gas over the fire. This volume is also a region of high concentrations of carbon monoxide, carbon dioxide, water vapor and a deficit region of oxygen. After the bubble becomes sufficiehtly hot to overcome the surface drag forces, a vortex ring forms which rises to a level of vertical wind shear sufficient to form a couple to rotate the vortex about a horizontal axis. The convection column decelerates rapidly and moves horizontally with the wind. With the exception of the levels just above the fire, there is little exchange between the ambient air and large fire convection column because of the strong line vortex pairs generated by the fire.

Smoke from these fires consists of solid particles of carbon and soil mixed with semi-liquid and liquid particles of complex sugars and tars formed by the combination of the fuels absorbed water and water of combustion with the volatile hydrocarbons from the pyrolytic breakdown of the wood. These particles are probably hygroscopic and in equilibrium with the ambient humidity.

Inside even moderate sized fires, wind may be in excess of 70 m s^{-1} which can loft significant quantities of mineral and fine fuel residues to 1000 m or more. When a large 'fire storm' forms, all dense movable materials less than 1 cm dia. such as sand and small gravel was deposited at some distance.

The rates of production of smoke and convection column phenomenology described above should form a basis for estimating the degradation of air quality and visibility from large open fire, but information about the hygroscopisity of combustion products such as tars and sugars will be required to describe long term effects and transport.

REFERENCES

Benech B. (1976) Experimental study of an artificial convective plume initiated from the ground. *J. appl. Met.*, **15**, 127–137.

Church C. R., Snow J. T. and Dessens J. (1980) Intense atmospheric vortices associated with a 1000 MW fire. *Bull. Am. met. Soc.*, **61**, 682–694.

Lhermitte R. M. (1969) Note on the observation of small-scale atmospheric turbulence by Doppler radar techniques. *Radio Sci.* **4**, 1242–1246.

Morton B. R., Taylor G. and Turner J. S. (1956) Turbulent gravitational convection from maintained and instantaneous sources. *Proc. R. Soc.* (*A*), **234**, 1–23.

Murray J. R., Northcutt L. I. and Countryman C. M. (1971) Measuring mass loss rates in free burning fires. *Fire Technol.*, **7**, 162–169.

Palmer T. Y. (1971) Comparison of aspirated and radiation compensating thermocouples. *Fire Technol.*, **6**, 224–228.

Palmer T. Y. (1975) Convection columns above large fires. *Fire Technol.*, **11**, 111–118.

Palmer T. Y. (1976) Adsorption by smoke particles of thermal radiation in large fires. *J. Fire Flam.*, **7**, 460–469.

Palmer T. Y. and Northcutt L. I. (1972) A high temperature water-cooled anemometer. *Fire Technol.*, **7**, 201–204.

Tennekes H. and Lumley J. L. (1972) *A First Course in Turbulence*, pp. 271–273. MIT Press, Cambridge, Mass.

Turner J. S. (1973) *Buoyancy Effects in Fluids*, pp. 189–191. Cambridge University Press, London.

Williams D. W., Adams J. S., Batten J. J., Whitty G. F. and Richardson G. T. (1970) Operation Euroka, an Australian Mass Fire Experiment, Report 386, Defence Standards Lab., Maribyrnon, Victoria, Australia.